16 Heat and Fluid Flow of Gases in Porous Media with Micropores: Slip Flow Regime

Moghtada Mobedi, Murat Barisik, and A. Nakayama

CONTENTS

16.1 INTRODUCTION

Heat and uid ow in porous media have found wide applications ranging from nature to industry. The ow of air into a human lung, ow of water in soil, uid ow in underground geothermal elds, ow of crude oil in underground reservoirs, and even air ow between tree trunks in forests are some examples of transport in a porous environment. The ow of hot air for drying in xed packed beds, the use of metal foams to enhance heat transfer, and uid ow in membranes are examples of industrial applications. Due to these extensive uses, the number of studies that focuses on porous transport eld has increased exponentially in recent years.

The mechanism of heat and uid transport through the pores is very complex such that determining the velocity, pressure, and temperature elds is a challenging task. There are two main theoretical approaches to analyze heat and uid ow in a porous structure known as pore scale method (PSM) and volume-averaged method (VAM). In PSM, the conservation of mass and momentum is solved for the uid owing through the voids of the porous medium. The energy equation can be solved for both solid and uid ow in the pores to nd temperature eld both in solid and uid regions. The PSM yields accurate distributions for velocity, pressure, and temperature. However, its practical application on porous media, which are generally heterogeneous with numerous pores and voids, is troublesome. This dif culty with PSM leads researchers to develop and employ VAM. VAM is developed based on volume average theory. The results of VAM may not provide an exact view for temperature, pressure, and velocity in the porous media since spaced-averaged values are used. However, the method is practical and the accuracy of results is generally in acceptable ranges. Porous media consists of solid and uid phases considered as a continuum domain and the heat and

uid ow equations are established for this imaginary continuum domain. Establishment of VAM governing equations requires the de nition of the volume average velocity, pressure, and temperatures as main dependent variables. Taking volume integral of the continuity, momentum and energy equations over a representative elementary volume (REV) of a porous structure results in additional unknown parameters such as permeability, Forchheimer coef cient, interfacial heat transfer coefcient, and thermal dispersion coef cients. These parameters are known as VAM transport parameters and the application of VAM requires the knowledge of values of VAM transport parameter. The values of permeability tensor depend on the geometrical parameters of the porous media. However, the values of Forchheimer, interfacial convective heat transfer coef cient, and thermal dispersion tensor depend on geometrical parameters, character of ow in the pores, etc. It should be mentioned that, recently, Nakayama et al. [1] showed that in addition to the aforementioned macroscopic transport properties, thermal tortuosity also plays an important role in determining an accurate temperature eld in porous media. Consequently, a VAM transport parameter relating to thermal tortuosity should also be added to the aforementioned unknown transport parameters.

The two methods for determining VAM transport parameters are the experimental and theoretical methods. Determination of permeability and thermal dispersion by experimental methods were discussed in the review studies of Sharma and Siginer [2] and Ozgumus et al. [3] in detail. Pore scale simulation of heat and uid ow for a REV of the porous media has become popular in recent years due to developments both in computer technology and computational methods. Multiple studies on pore scale simulation of heat and uid ow in porous media can be found in the literature. For heat and uid ow in isotropic periodic porous media, examples such as the studies of Nakayama et al. [4] on 2D porous media with square rods, Saito and de Lemos [5] on the determination of interfacial heat transfer coef cient for 2D porous media with square rods, and Nakayma and Kuwahara [6] on the modeling of 3D PSM for a regular and periodic porous media can be given. For nonisotropic but periodic porous media structure, studies were conducted by Ozgumus and Mobedi [7] for 2D porous media with rectangular rods and Nakayama et al. [8] for 2D porous media with different directional cell. For real heterogeneous porous media that can be represented in computer environment by using methods such as tomography or MRI, the studies of Peszynska and Trykozko [9], Akolkar and Petrasch [10], and Ucar et al. [11] should be noted.

The aforementioned studies were performed to determine VAM transport properties for porous media of pore sizes greater than micron scales in which gas ows at standard conditions permit the use of continuum assumptions and constitutive laws. However, there exist many porous media with micron-scale pores (such as micro ltration devices, packed beds with micron-scale particles, or micron-scale size ber porous structure) and low-pressure environments (vacuum absorption applications) where nonequilibrium gas behavior develops known as the rarefaction. Most of the existing correlations suggested for the determination of VAM transport properties are developed without considering this rarefaction effect and may not be valid for the porous media having pores in micron scale and/or operated under low pressures. For such cases, the Knudsen number de ned as the ratio of mean free path to the characteristic length is employed as a measure of the degree of rarefaction. For a certain level of rarefaction, Navier–Stokes equations are found to be valid with slip boundary conditions. Also known as the slip ow regime, Maxwell de ned that velocity slip and temperature jump conditions can incorporate the rarefaction formed as a result of small scale and/or low pressure. New correlations or diagrams for the determination of VAM transport properties should be investigated or the suggested correlations in literature should be revised as a function of rarefaction.

Literature survey showed that the number of PSM studies examining the VAM transport parameters of porous media with microchannels is limited compared to studies performed for macro channels. Most of the previous studies are on the determination of permeability rather than thermal VAM transport properties, such as the study of Jeong [12] in which lattice Boltzmann method was used to determine the permeability for microporous structures. For thermal VAM transport properties, the study of Vu et al. [13] on forced convection of air through networks of square rods or

cylinders can be given as an example. They found permeability values for 2D porous media with staggered squared rods. Furthermore, Kuwahara et al. [14] studied the heat and uid ow for 2D porous media with square rods and microscale channels and determined the values of permeability and tortuosity. Xu et al. [15] studied the rare ed effects on internal heat transfer coef cients in microporous media for sintered bronze porous media with average particle diameters from 11 to 225 μm.

The aim of the present work is to perform a numerical study on 2D porous media consisting of square rods in micron size in order to determine VAM transport properties, including permeability and interfacial heat transfer coef cient in slip ow regime. Brief information on the VAM motion and heat transfer equations and the concept of heat and uid ow in microscale channel with rarefaction effect in slipping region is provided. Then, the obtained results for permeability and interfacial heat transfer coef cient are presented for a 2D porous medium.

16.2 VAM MOTION AND HEAT TRANSFER EQUATIONS

A porous medium consists of solid particles and the voids between solid particles are shown in Figure 16.1. In order to obtain the pore scale temperature, velocity, and pressure elds, an REV is considered in the porous medium, then continuity, momentum and energy equations can be solved for the considered REV.

If a steady-state single phase and incompressible uid ow exists in the voids between particles, the governing equations can be expressed as

$$\begin{aligned}
&\vec{\nabla}\cdot\vec{V}=0\\
&\left(\vec{\nabla}.\vec{V}\right)\vec{V}=-\frac{1}{\rho}\vec{\nabla}p+\nu\vec{\nabla}^2\vec{V}\\
&(\rho c_p)_f(\vec{V}.\vec{\nabla})T_f=k_f\vec{\nabla}^2T_f\\
&\vec{\nabla}^2T_s=0
\end{aligned}\tag{16.1}$$

The solution of these equations with appropriate boundary conditions yields velocity, pressure, and the solid and uid phase temperature distributions for the REV of porous media. For an isotropic porous media, the obtained microscopic results are valid for the entire porous media. For nonisotropic or heterogeneous porous media, different REVs at different locations should be considered.

For VAM, the porous medium consists of solid and voids in which the uid owing is replaced by an imaginary continuum medium. The derivation of VAM-governing equation requires the

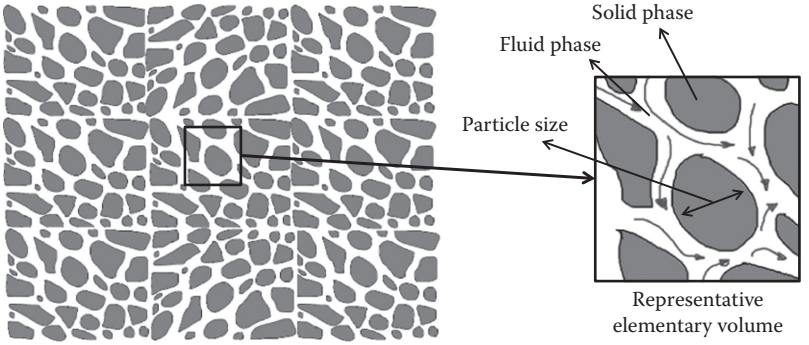

FIGURE 16.1 The illustration of a porous medium and considered representative elementary volume (REV).

de nition of volume average. For an REV shown in Figure 16.1, two types of volume average as total volume average of quantity φ and the intrinsic volume average value of φ can be de ned.

$$\langle \varphi \rangle = \frac{1}{V}\int_V \varphi \, dV$$
$$\langle \varphi \rangle^x = \frac{1}{V_x}\int_{V_x} \varphi \, dV \tag{16.2}$$

where

V is the total volume of REV

V_x is the volume of considered phase in REV (s or f stands for solid or uid phases, respectively).

The variable of φ can be velocity, pressure, or temperature in the present study. The following relation exists between the values of real and volume averaged of quantity of φ:

$$\langle \varphi \rangle = \varphi - \varphi' \tag{16.3}$$

where φ′ refers to the deviation of volume-averaged value from the real value of φ for any location in REV. Taking volume integral from the continuity, momentum, and energy equations over the REV and neglecting thermal tortuosity effect in REV yield the macroscopic motion and energy equations:

$$\vec{\nabla}\cdot\langle \vec{V} \rangle = 0$$
$$\frac{1}{\varepsilon}\frac{\partial \langle \vec{V} \rangle}{\partial t} + \frac{1}{\varepsilon^2}\left(\langle \vec{V} \rangle \cdot \vec{\nabla}\right)\langle \vec{V} \rangle = -\frac{1}{\rho_f}\nabla \langle p \rangle^f + \frac{\nu}{\varepsilon}\nabla^2 \langle \vec{V} \rangle - \frac{\mu}{\rho_f K}\langle \vec{V} \rangle - \frac{C}{K^{1/2}}\left|\vec{V}\right|\vec{V}$$
$$(\rho c_p)_s (1-\varepsilon)\frac{\partial \langle T \rangle^s}{\partial t} = k_s (1-\varepsilon)\vec{\nabla}^2 \langle T \rangle^s + h_{sf}\frac{A_{sf}}{V}\left(\langle T \rangle^s - \langle T \rangle^f\right) \tag{16.4}$$
$$(\rho c_p)_f \varepsilon \frac{\partial \langle T \rangle^f}{\partial t} + \rho_f c_{p_f}\langle \vec{V} \rangle \cdot \nabla \langle T \rangle^f = k_f \varepsilon \vec{\nabla}^2 \langle T \rangle^f + h_{sf}\frac{A_{sf}}{V}\left(\langle T \rangle^s - \langle T \rangle^f\right) + k_{dis}\vec{\nabla}^2 \langle T \rangle^f$$

where

$\langle \vec{V} \rangle$ is the local average velocity

$\langle p \rangle^f$ and $\langle T \rangle^f$ are the intrinsic average pressure and temperature of the uid phase while $\langle T \rangle^s$ is the average temperature in the solid phase in REV

If these equations are compared with the pore-level governing equations, it can be seen that there are new terms in the VAM transport equation involving new parameters called as VAM transport parameters. The new unknown VAM transport parameters are K, h_{sf}, C, and k_{dis} named as

permeability, interfacial heat transfer coefficient, Forchheimer coefficient, and thermal dispersion coefficient, respectively. As mentioned previously, these macroscopic transport parameters should be known in order to obtain volume-averaged temperature, velocity, and pressure fields.

16.3 HEAT AND FLUID FLOW IN MICROSCALE CHANNELS

The effect of pore size along with gas pressure is especially important since most of the porous media contains sub-micron-size pores in addition to existing low-pressure vacuum absorption applications. As the pore size becomes comparable to the mean free path of the gas molecules, nonequilibrium gas behavior occurs known as the rarefaction effects leading to the breakdown of the continuum assumptions and constitutive laws.

Nonequilibrium gas flows are classified by the Knudsen number (Kn = λ/H), which is the ratio of the local gas mean free path (λ) to the characteristic length scale (H), such as the channel height or pore size. Depending on Kn, transport is considered in the continuum (Kn $\leq$ 0.01), slip (0.01 $\leq$ Kn $\leq$ 0.1), transition (0.1 $\leq$ Kn $\leq$ 10), and free-molecular (Kn > 10) flow regimes [16]. Within the context of continuum fluid dynamics, constitutive laws used in the definition of stress tensor and heat flux vector and the no-slip boundary condition break down with increased Knudsen number. For example in a 1 μm conduit, gas at standard pressure and temperature develops transport in the slip flow regime. For such cases, the continuum no-slip boundary condition becomes invalid due to gas rarefaction, but the Navier–Stokes equations can still be employed with an appropriate boundary conditions defined on the surface. The fluid particles adjacent to the boundary surface are not in thermodynamic equilibrium with the wall that there would be slip velocity and temperature jump at the channel wall (For a more detailed discussion on these, readers are referred to the textbook by Gad-el-Hak [17]). For the slip flow regime (0.01 < Kn < 0.1), slip velocity and temperature jump boundary conditions for a microtube can be defined as follows [18]:

$$u_n = -\frac{2-\sigma_m}{\sigma_m}\lambda\left.\frac{\partial u}{\partial n}\right|_{wall} \tag{16.5}$$

$$T_f - T_w = -\frac{2-\sigma_t}{\sigma_t}\frac{2\gamma}{\gamma+1}\frac{\lambda}{Pr}\left.\frac{\partial T_f}{\partial y}\right|_{wall} \tag{16.6}$$

where

σ_m is the tangential momentum accommodation coefficient
σ_t is the thermal accommodation coefficient
γ is the specific heat ratio

These slip flow models are successfully employed to consider the effect of rarefaction on microscale flow [19] while good agreements are obtained with experimental measurements [20].

16.4 THE CONSIDERED TWO-DIMENSIONAL POROUS MEDIA

The schematic of the considered porous medium is shown in Figure 16.2. The porous medium is an infinite media consisting of square rods in inline arrangement. Considering the periodicity of the porous structure, an REV with the dimensions $H \times H$ is employed to investigate the effect of Knudsen number on permeability and interfacial convective heat transfer coefficient. The dimension of the REV and the square blocks are constant for all studied cases. The height of REV (i.e., H) is 670 μm while the size of square block (i.e., D) is 335 μm. The porosity of porous media is unchanged and the constant is $\varepsilon = 0.75$.

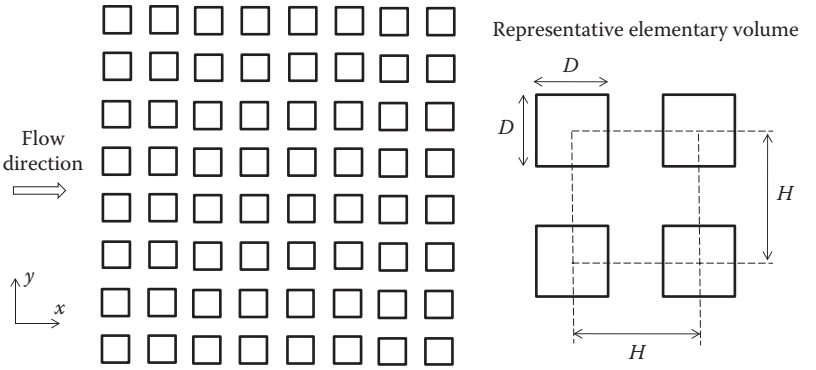

FIGURE 16.2 The studied 2D porous media.

TABLE 16.1
Cases Studied for the Determination of Permeability (T = 300 K)

Cases Studied	Pressure (Pa)	Density (kg/m^3)	Mean Free Path (μm)	Knudsen Number
Case 1	101325	1.17659	6.70006E−08	0.0001
Case 2	10132.5	0.11766	6.70006E−07	0.001
Case 3	1013.25	0.011766	6.70006E−06	0.01
Case 4	506.625	0.005883	1.34001E−05	0.02
Case 5	202.65	0.002353	3.35003E−05	0.05
Case 6	101.325	0.001177	1.177000E−03	0.10

The uid owing through the porous media is air. For determination of permeability for the considered porous media, the dynamic viscosity of air is taken as 18.21 × 10^{-6} kg/ms. The air pressure is changed from 101325 to 101.325 Pa while its temperature is constant at 300 K. Based on the assumed temperature and pressure, the air density changes and different mean free path and consequently different Knudsen number are achieved. Table 16.1 shows the studied cases with corresponding density, mean free path, and Knudsen number. As shown in Table 16.1, in order to investigate permeability change with Knudsen number, six cases are studied. It should be mentioned that the permeability values are obtained in very low Re number as 0.001 to remove the inertia effect in the ow eld.

In order to calculate the interfacial convective heat transfer coef cient, the solid particle is assumed at constant temperature of 310 K. A study is performed for two Reynolds numbers of 10 and 100 and six cases are considered for each Re number. The density of the air and mean free path are calculated according to the mean temperature which is the arithmetic average of periodic inlet and outlet temperatures and surface temperature.

16.5 GOVERNING EQUATIONS, BOUNDARY CONDITIONS, AND SOLUTION METHOD

The ow in the voids between the particles is assumed incompressible and steady. The uid (i.e., air) is Newtonian uid with constant thermophysical properties. The steady form of the continuity and momentum equations (Equation 16.1) is solved to determine the velocity and pressure elds for the uid ow in the voids between the blocks. After obtaining the velocity eld in the porous media, the energy equation for uid phase is solved to obtain the temperature distributions in

the REV. Considering REV in Figure 16.2, the boundary conditions for the microscopic equations are chosen as symmetry for the top and the bottom of the REV. The periodic velocity and temperature pro les are used for the inlet and outlet boundaries. The velocity and temperature gradients at the outlet boundary are assumed zero, hence no diffusion transport exists. The discretization interval is chosen as 0.02 mm which makes the number of grids as 500 × 500 for the entire domain. The Fluent commercial code based on the nite volume method is used to solve the governing equations. SIMPLE method is used for handling the pressure–velocity coupling. The power law scheme is employed for the discretization of the convection terms in the momentum and energy equations. The approximate errors are set to 10^{-9} for ow equations and 10^{-12} for temperature eld.

16.5.1 Calculation of Permeability

As it is well known, permeability is a tensor quantity and based on Darcy's law for a 2D ow in Cartesian coordinate, and it can be de ned as

$$\begin{pmatrix} \langle u \rangle \\ \langle v \rangle \end{pmatrix} = \frac{1}{\mu} \begin{pmatrix} K_{xx} & K_{yx} \\ K_{xy} & K_{yy} \end{pmatrix} \begin{pmatrix} \dfrac{\partial p}{\partial x} \\ \dfrac{\partial p}{\partial y} \end{pmatrix} \tag{16.7}$$

where K_{xy}, K_{yx}, K_{xy}, and K_{xy} are components of the permeability tensor. In the present problem, the permeability is calculated only for x direction since the structure of porous media is symmetrical not only in x and y directions but also with respect to xy and yx diagonals. The permeability is calculated based on velocity and pressure elds obtained from the continuity and momentum equations. Considering the REV shown in Figure 16.2, the following boundary conditions are used with σ_m=1 assumption:

$$\begin{aligned} &\text{On solid walls:} \quad u_n = -\lambda \left.\frac{\partial u}{\partial n}\right|_{wall} ; \quad u_t = 0 \\ &\text{For inlet boundary:} \quad u(0,y) = f(y),\ v(0,y) = 0 \\ &\text{For outlet boundaries:} \quad \frac{\partial u(H,y)}{\partial x} = \frac{\partial v(H,y)}{\partial x} = 0 \end{aligned} \tag{16.8}$$

where u_n and u_t are normal and tangential components of the velocity vector at the solid wall and they can be u or v components according to the position of wall. The mean free path is shown by λ in the earlier equation. The pro le velocity of $f(y)$ is obtained by an iterative procedure. A uniform velocity distribution is assigned for the inlet velocity, and the outlet velocity is obtained by solving the continuity and momentum equations according to the aforementioned boundary conditions. Then, the obtained outlet velocity is used as inlet velocity pro le and the same equations are solved again. The procedure continues until the inlet and outlet velocity pro les become identical (i.e., $f(y)$).

The Darcy velocity and pressure gradient in x direction for ow through the REV are calculated by the following relation:

$$\langle u \rangle = \frac{1}{H^2} \int_0^H \int_0^H u \, dx \, dy \tag{16.9}$$

$$\frac{d\langle p\rangle^f}{dx} = -\frac{1}{H(H-D)}\left[\int_{D/2}^{H-D/2} p\big|_{x=0}\,dy - \int_{D/2}^{H-D/2} p\big|_{x=H} dy\right] \tag{16.10}$$

Hence the permeability for x direction can be obtained from the following Darcy equation:

$$\langle u_f\rangle = -\frac{k_{xx}}{\mu}\frac{d\langle p\rangle^f}{dx} \tag{16.11}$$

Considering Figure 16.2, the permeability tensor for the present problem takes the following form:

$$\begin{pmatrix}\langle u_f\rangle\\ \langle v_f\rangle\end{pmatrix} = \frac{1}{\mu}\begin{pmatrix}K_{xx} & 0\\ 0 & K_{yy}\end{pmatrix}\begin{pmatrix}\dfrac{\partial p}{\partial x}\\ \dfrac{\partial p}{\partial y}\end{pmatrix} \tag{16.12}$$

For the studied cases, the values of K_{xx} and K_{yy} are equal to each other due to symmetrical geometry of REV.

16.5.2 Calculation of Interfacial Heat Transfer Coefficient

For a thermal nonequilibrium condition, the heat transfer between the solid phase surface and the uid owing in the voids can be calculated by using the interfacial convective heat transfer concept. Mathematically, the convective heat transfer between the solid and uid can be calculated by the following relation:

$$h_{sf}A_{ss}(\langle T_s\rangle - \langle T_f\rangle) = \frac{k_f}{V}\int_{A_{sf}} \vec{n}\cdot\vec{\nabla}T\,dA \tag{16.13}$$

where

h_{sf} is the interfacial convective heat transfer coef cient
A_{sf} is the solid– uid interface area
A_{ss} is the speci c solid– uid interface area (i.e., $A_{ss} = A_{sf}/V$).

Correspondingly, the interfacial Nusselt number can be de ned as follows:

$$\mathrm{Nu}_{sf} = \frac{h_{sf}H}{k_f} \tag{16.14}$$

where H represents the length and height of the REV. Although different characteristic lengths such as hydraulic diameter and the block height may be employed to de ne Nusselt number for the studied porous structure, the dimension of the REV is selected in this study. The same characteristic

length is also selected in many reported studies [4,5,7]. Considering the REV in Figure 16.2, the thermal boundary conditions for the PSM equations are as follows:
On the solid walls

$$T_f - T_w = -\kappa\lambda \left.\frac{\partial T_f}{\partial y}\right|_{wall}$$

On the top and bottom

$$\frac{\partial T_f}{\partial y} = 0$$

For inlet boundary

$$T(0, y) = g(y) \tag{16.15}$$

For outlet boundary

$$\frac{\partial T_f}{\partial x} = 0$$

where κ is a parameter that represents the degree of temperature jump, de ned from the temperature jump boundary condition, $\kappa = ((2-\sigma_t)/\sigma_t)(2\gamma/(\gamma + 1))(1/\mathrm{Pr})$, and κ = 0 corresponds to no temperature jump at the wall, while κ = 1.667 is a typical value for air, which is the working uid in many engineering applications and is taken so in this study. As seen in Equation 16.15, a temperature jump is assumed at the interface between the solid and uid phases. The function of $g(y)$ is the temperature pro le that provides thermal periodicity for the inlet and outlet boundaries of the REV. In order to determine the function of $g(y)$, it is assumed that a thermally fully developed convection heat transfer is valid which means that no change of the dimensionless temperature should be observed in sequential REVs in the ow direction. A uniform temperature pro le which is different from the solid temperature is de ned for the uid inlet boundary and then the temperature eld for the entire domain and consequently for the outlet boundary is obtained. The temperature at the inlet is determined from the dimensionless temperature pro le at the outlet boundary. The iterative process continues until no change in the dimensionless temperature distribution at the inlet and outlet is observed. The dimensionless temperature equality for achieving thermally periodic ow is

$$\left.\frac{T - T_w}{T_b - T_w}\right|_{inlet} = \left.\frac{T - T_w}{T_b - T_w}\right|_{outlet} \tag{16.16}$$

where T_b is the bulk temperature and it can be obtained by the following relation for the considered REV:

$$T_b = \frac{\int_A uT dA}{\int_A dA} \tag{16.17}$$

Furthermore, following dimensionless temperature distribution is de ned to provide temperature distribution of different REV in the same range:

$$\theta^* = \frac{T - T_{\min}}{T_{\max} - T_{\min}} \tag{16.18}$$

where T_{min} and T_{max} are the minimum and maximum temperatures in the considered temperature field.

16.6 RESULTS AND DISCUSSION

In this section, the results for permeability and interfacial heat transfer coefficient are presented separately.

16.6.1 Permeability

As discussed previously, a commercial code is used to solve the microscopic governing equations for the considered porous media. In order to define slipping boundary conditions for solid walls, a user defined function (UDF) is written and adapted to program. The validation of written UDF is checked with fully developed velocity profiles in a channel obtained analytically. Figure 16.3 shows the dimensionless velocity profile obtained by the employed code and the corresponding analytical results for a straight channel for three different Knudsen numbers. As shown, there is a good agreement between the analytical solution and the obtained computational results illustrating the correctness of the written UDF code.

Figure 16.4 shows the distribution of longitudinal dimensionless velocity component for two Knudsen numbers of 0.0001 and 0.1. The dimensionless velocity is defined as the ratio of velocity component to the mean inlet velocity value. A high-velocity gradient at the solid horizontal surface for Kn = 0.0001 can be observed. By increasing the Knudsen number from 0.0001 to 0.1, the gradient of velocity at the solid surface decreases considerably and this causes a lower pressure drop through the REV. Hence, it may be expected that the increase in Knudsen number increases the permeability of fluid through the porous medium. The values of permeability for the cases given in Table 16.1 are obtained and nondimensionalized with H^2. The results are presented in Figure 16.5.

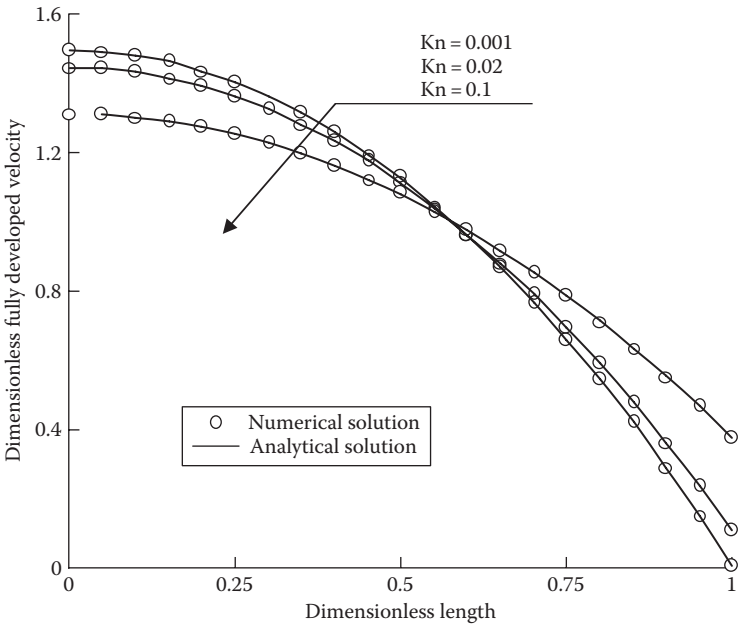

FIGURE 16.3 Comparison of computational results with the analytical solution.

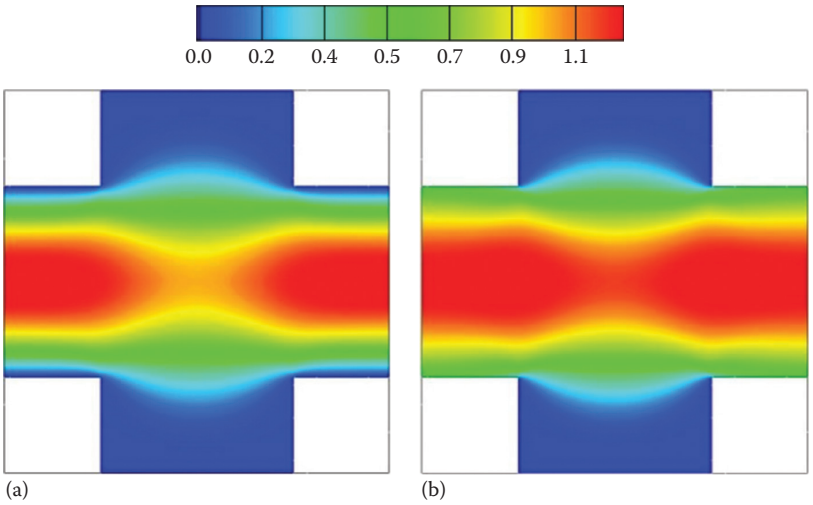

FIGURE 16.4 Distribution of dimensionless longitudinal velocity component for ow in REV: (a) Kn = 0.0001 and (b) Kn = 0.1.

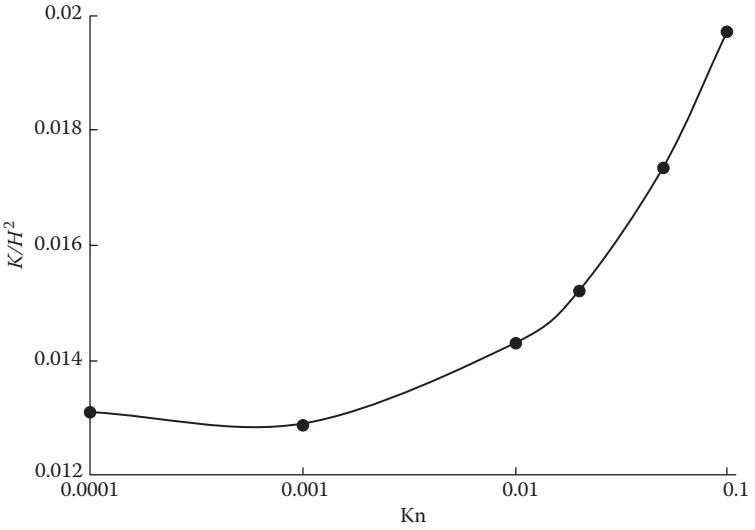

FIGURE 16.5 The change of dimensionless permeability with Kn number.

The permeability value increases considerably with Knudsen number indicating high permeability at lower Knudsen number.

Although many equations were suggested in the literature for the determination of permeability under rare ed effect, it seems that the relationship presented by Kuwahara and Nakayama [14] is the most suitable equation for the studied porous media in this work.

$$\frac{K}{K_{ns}} = 1 + C\,\mathrm{Kn} \tag{16.19}$$

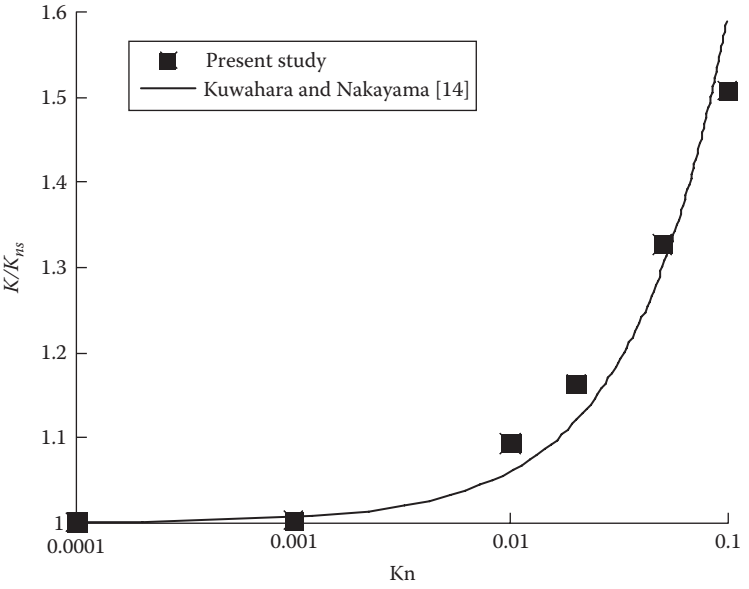

FIGURE 16.6 The comparison between the obtained numerical results with the correlation suggested by Kuwahara and Nakayama [14].

where K_{ns} is the permeability of the porous media for no-slip boundary condition. The coef cient of C is de ned as

$$C = 9\frac{(1-\varepsilon)^{1/2}}{\varepsilon} \tag{16.20}$$

Figure 16.6 shows the comparison of the obtained results with correlation suggested by Kuwahara and Nakayama. As shown, good agreement between the correlation and the numerical results obtained in this study is observed.

16.6.2 Interfacial Convective Heat Transfer

Similar to the calculation of permeability, UDF codes are written to provide temperature jump for horizontal and vertical interfaces between solid and uid boundaries. The written code and program are checked by comparing numerical results with Refs. [21,22] for a channel and it is shown in Figure 16.7. A good agreement between the computational results of present and reported studies can be observed.

Figure 16.8 shows the dimensionless temperature distribution for two porous media with two different Reynolds and Knudsen numbers. Figure 16.8a shows the temperature contours in porous media for Re = 10. It should be mentioned that the dimensionless temperature at the solid– uid is 1 (i.e., $\theta^* = 1$). For Kn = 0.0001, the temperature of uid at the region close to the solid surface is around 1 (i.e., $\theta^* = 1$) due to negligible temperature jump at the solid surface. By increasing Kn number from 0.0001 to 0.1, the effect of the slipping boundary condition can be observed clearly. The interface temperature for uid region is considerably reduced and this causes uid owing in

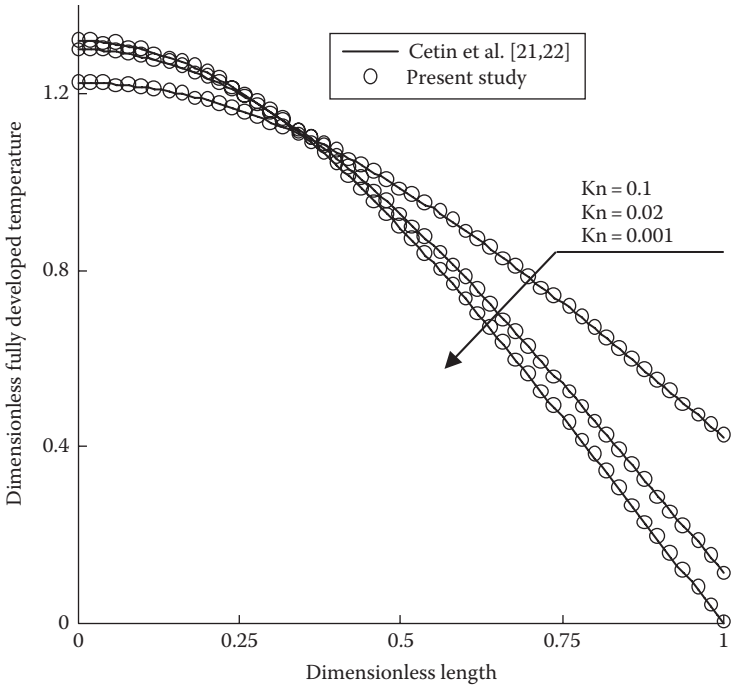

FIGURE 16.7 Comparison of obtained computational and reported temperature pro les for a straight channel.

the voids which cannot be heated. Figure 16.8b shows the same porous media; however, the Re number is increased to 100. The same behavior for temperature changes observed for Re = 10 can also be seen for uid owing in the voids with Re = 100. The Kn number has an important effect on the temperature eld of uid and it reduces the heat transfer rate in the voids. Hence, a reduction in interfacial heat transfer coef cient is expected.

The change in interfacial Nusselt number with Knudsen for two Reynolds number of Re = 10 and 100 is presented in Figure 16.9. As expected, the Nu number considerably decreases with Kn number for both Re = 10 and 100 ows. The interesting point of Figure 16.9 is that the difference between Nu number of ows with Re = 10 and 100 depends on the Kn number. By increasing Kn number, the difference between Nu numbers is reduced.

Our study shows that it is possible to express a relation for interfacial heat transfer coef cient based on no-slip Nusselt number. A relation for the determination of Nu_{sf} for porous media with $\varepsilon = 0.75$ is found as follows:

$$\frac{Nu_{sf}}{Nu_{ns,sf}} = 0.9915 - 11.757Kn + 57.83Kn^2 \tag{16.21}$$

where $Nu_{ns,sf}$ is the interfacial Nusselt number for porous media with no-slip boundary condition. Figure 16.10 shows the comparison of the suggested relation with the obtained numerical results.

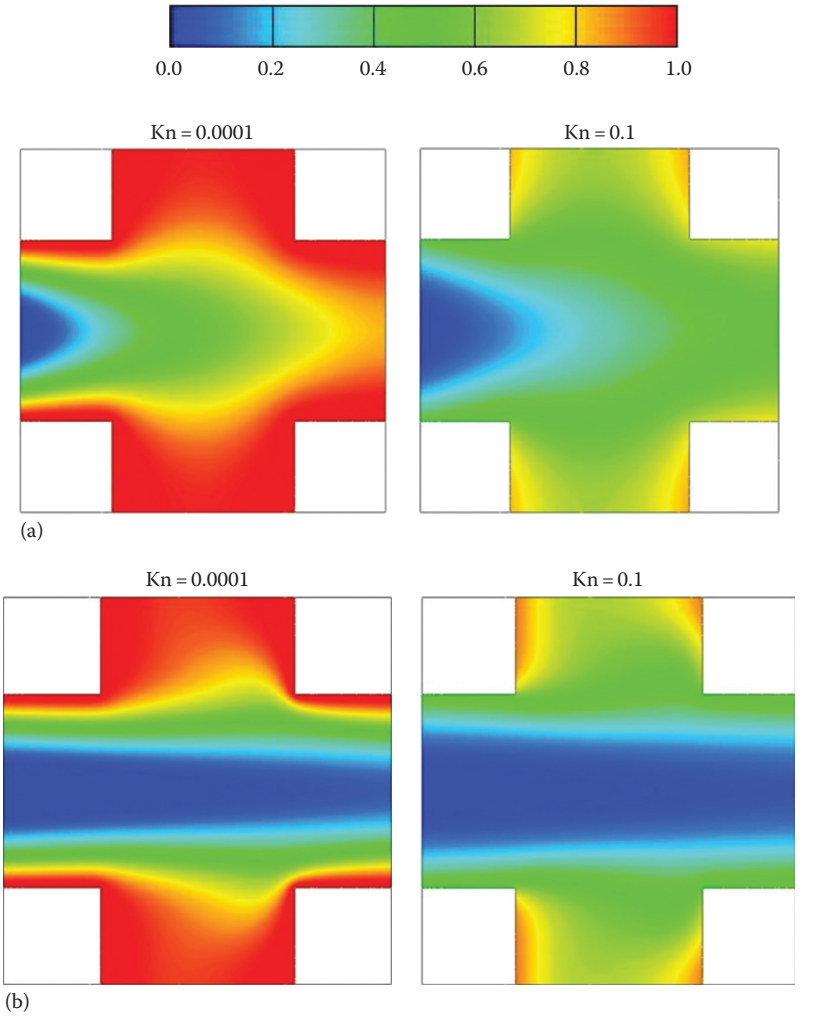

FIGURE 16.8 Dimensionless temperature distribution in the porous media: (a) Re = 10 and (b) Re = 100.

16.7 CONCLUSION

A numerical study on heat and uid ow in a 2D porous media with microchannel is performed. The related PSM-governing equations and boundary conditions are solved and both permeability and interfacial heat transfer coef cient are calculated by using volume-averaged method. It is observed that for porous media with microchannel particularly at low gas pressure, the Kn number has a signi cant effect on both permeability and interfacial heat transfer coef cient. Hence, the traditional corrections reported in the literature for permeability and interfacial heat transfer coef cient cannot be used. Two-dimensional porous media studies showed that an increase in Kn number from 0.0001 to 0.1 increased the permeability by 51%. The reduction of interfacial heat transfer coef cient with Kn number depends on Re number. The interfacial heat transfer coef cients become closer to each other with an increase in the Kn number.

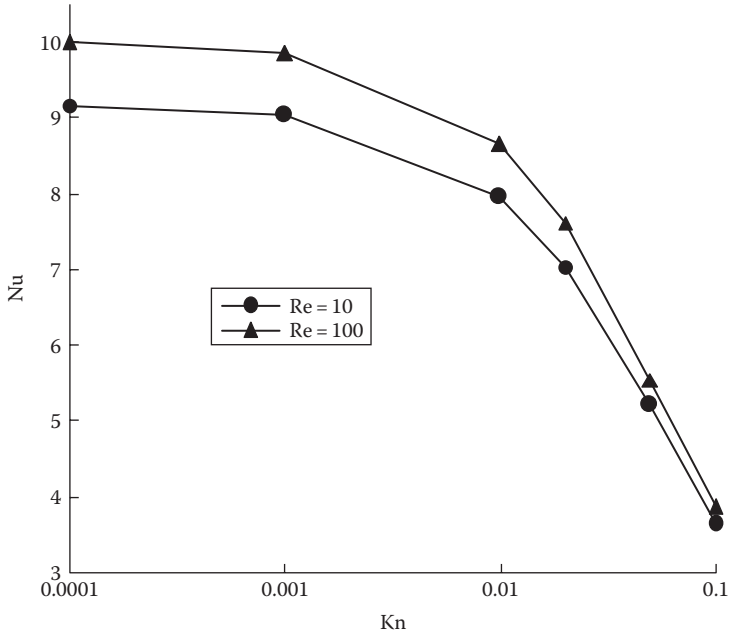

FIGURE 16.9 The change in Nu number with Kn for two Re numbers of 10 and 100.

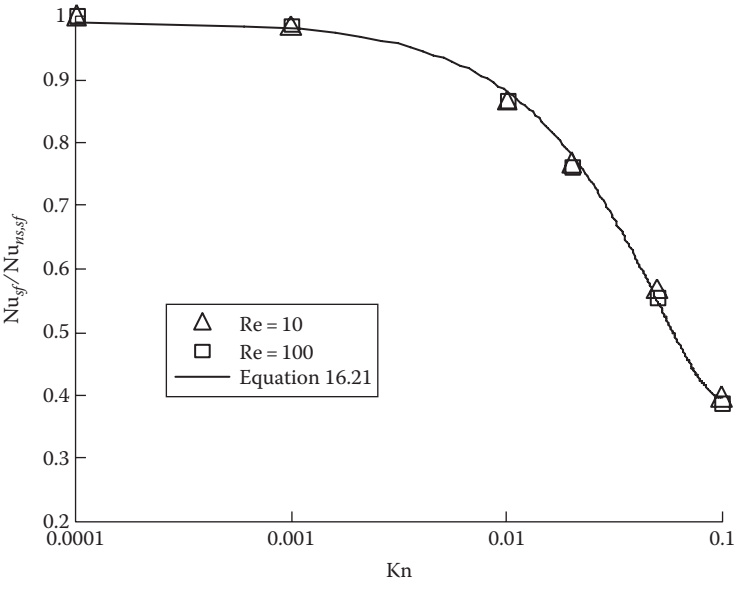

FIGURE 16.10 Comparison of the suggested correlation with obtained numerical results.

ACKNOWLEDGMENT

The authors want to thank M.Sc. student Safa Sabet for his great effort in obtaining computational results and it would have been dif cult to nish this study on time without his help.

REFERENCES

1. C. Yang, A. Nakayama, A synthesis of tortuosity and dispersion in effective thermal conductivity of porous media, *Int. J. Heat Mass Transfer*, 53 (15), 3222–3230 (2010).
2. S. Sharma, D.A. Siginer, Permeability measurement methods in porous media of ber reinforced composites, *Appl. Mech. Rev.*, 63 (2), 020802–020802-19 (2010).
3. T. Ozgumus, M. Mobedi, U. Ozkol, A. Nakayama, Thermal dispersion in porous media; a review on the experimental studies for packed beds, *Appl. Mech. Rev.*, 65 (3), 031001–031001-19 (2013).
4. F. Kuwahara, A. Nakayama, Numerical determination of thermal dispersion coef cients using a periodic porous structure, *J. Heat Transfer*, 121 (1), 160–163 (1999).
5. M.B. Saito, M.J.S. de Lemos, A correlation for interfacial heat transfer coef cient for turbulent ow over an array of square rods, *J. Heat Transfer*, 128, 444–452 (2006).
6. A. Nakayma, F. Kuwahara, Numerical modeling of convective heat transfer in porous media using microscopic structure, *Hand Book of Porous Media*, Edited by Vafai K., Marcel Dekker Inc., New York, pp. 441–487 (2000).
7. T. Ozgumus, M. Mobedi, Effect of pore to throat size ratio on interfacial heat transfer coef cient of porous media, *J. Heat Transfer*, 137 (1), 012602 (2014).
8. A. Nakayama, F. Kuwahara, T. Umemoto, T. Hayashi, Heat and uid ow within an anisotropic porous medium, *J. Heat Transfer*, 124, 746–753 (2002).
9. M. Peszynska, A. Trykozko, Pore-to-core simulations of ow with large velocities using continuum models and imaging data, *Comput. Geosci.*, 17, 623–645, (2013).
10. A. Akolkar, J. Petrasch, Tomography-based characterization and optimization of uid ow through porous media, *Transp. Porous Med.*, 95, 535–550 (2012).
11. E. Ucar, M. Mobedi, G. Altıntas, E. Glatt, Effect of voxel size in ow direction on permeability and Forchheimer coef cients determined by using micro-tomography images of a porous medium, *Progress in Computational Fluid Dynamics* (in press).
12. N. Jeoong, Advanced Study about the permeability for micro-porous structures using the Lattice Boltzmann method, *Transp. Porous Med.*, 83, 271–288 (2010).
13. T.L. Vu, G. Lauriat, O. Manca, Forced convection of air through networks of square rods or cylinders embedded in microchannels, *Microfluid Nanofluid*, 16, 287–304 (2014).
14. F. Kuwahara, A. Nakayama, Numerical simulation of rare ed gas ow through a porous media, *Trans. Jpn. Soc. Mech. Eng.*, 69, 189–195 (1999).
15. R.N. Xu, Y.L. Huang, P.X. Jiyang, B.X. Wang, Internal heat transfer coef cients in microporous media with rarefaction effects, *Sci. China, Technol. Sci.*, 55 (10), 2869–2876 (2012).
16. A. Beskok, G.E. Karniadakis, Simulation of heat and momentum transfer in complex micro-geometries. *J. Thermophys. Heat Transfer*, 8, 355–370 (1994).
17. M. Gad-el-Hak, *The MEMS Handbook*, CRC Press, New York (2001).
18. G.E. Karniadakis, A. Beskok, N. Aluru, *Micro Flows and Nano Flows: Fundamentals and Simulation*, Springer-Verlag, New York, 2005.
19. H.P. Kavehpour, M. Faghri, Y. Asako, Effects of compressibility and rarefaction on gaseous ows in microchannels. *Numer. Heat Transfer, Part A,* 32, 677–696 (1997).
20. E.B. Arkilic, K.S. Breuer, M.A. Schmidt, Gaseous ow in microchannels. Application of microfabrication to uid mechanics. *ASME FED*, 197, 57–66 (1994).
21. B. Cetin, Analysis of single phase convective heat transfer in microtubes and microchannels, Master thesis, Middle East Technical University, 2005.
22. B. Cetin, H. Yuncu, S. Kakac, Gaseous ow in microchannels with viscous dissipation. *Int. J. Transp. Phenom.*, 8, 297–315 (2006).